A Conducting State with Properties of a Slow Inactivated State in a *Shaker* K^+ Channel Mutant

Riccardo Olcese,* Daniel Sigg,‡ Ramon Latorre,‖¶ Francisco Bezanilla,*‡§ and Enrico Stefani*‡§

From the *Department of Anesthesiology, ‡Department of Physiology, and §Department of Brain Research Institute, School of Medicine, University of California Los Angeles, Los Angeles, CA 90095; ‖Centro de Estudios Científicos,Valdivia, Chile; and ¶Departamento de Biología, Facultad de Ciencias, Universidad de Chile, Santiago, Chile

ABSTRACT In *Shaker* K^+ channel, the amino terminus deletion Δ6-46 removes fast inactivation (N-type) unmasking a slow inactivation process. In *Shaker* Δ6-46 (Sh-IR) background, two additional mutations (T449V-I470C) remove slow inactivation, producing a noninactivating channel. However, despite the fact that Sh-IR-T449V-I470C mutant channels remain conductive, prolonged depolarizations (1 min, 0 mV) produce a shift of the QV curve by about −30 mV, suggesting that the channels still undergo the conformational changes typical of slow inactivation. For depolarizations longer than 50 ms, the tail currents measured during repolarization to −90 mV display a slow component that increases in amplitude as the duration of the depolarizing pulse increases. We found that the slow development of the QV shift had a counterpart in the amplitude of the slow component of the ionic tail current that is not present in Sh-IR. During long depolarizations, the time course of both the increase in the slow component of the tail current and the change in voltage dependence of the charge movement could be well fitted by exponential functions with identical time constant of 459 ms. Single channel recordings revealed that after prolonged depolarizations, the channels remain conductive for long periods after membrane repolarization. Nonstationary autocovariance analysis performed on macroscopic current in the T449V-I470C mutant confirmed that a novel open state appears with increasing prepulse depolarization time. These observations suggest that in the mutant studied, a new open state becomes progressively populated during long depolarizations (>50 ms). An appealing interpretation of these results is that the new open state of the mutant channel corresponds to a slow inactivated state of Sh-IR that became conductive.

KEY WORDS: gating current • slow inactivation • C/P-type inactivation • nonstationary noise analysis

INTRODUCTION

In the absence of the fast N-type inactivation, the *Shaker* K^+ channel displays slow inactivation. Slow inactivation is one of the mechanisms by which ion channels become nonconducting during prolonged depolarization. In *Shaker* channels, it involves a cooperative conformational change of the channel subunits associated to rearrangements of the outer side of the pore (Yellen et al., 1994; Ogielska et al., 1995; Panyi et al., 1995; Liu et al., 1996; Basso et al., 1998; Loots and Isacoff, 1998). Slow inactivation (referred by different authors as C- or P-type) is mediated, at least in part, by amino acid residues in the S5-, P-, and S6-segments of the channel (Iverson and Rudy, 1990; Hoshi et al., 1991; López-Barneo et al., 1993; De Biasi et al., 1993; Olcese et al., 1997; Yang et al., 1997; Ogielska and Aldrich, 1998, 1999). This relatively slow process can also be revealed as a change in the voltage dependence of charge movement (QV) (also reported as charge immobilization or charge conversion) that takes place in slow inactivated channels. As described for Na^+ channels (Bezanilla et al., 1982), K^+ channels (Fedida et al., 1996; Olcese et al., 1997) and Ca^{2+} channels (Brum and Rios, 1987; Shirokov et al., 1992, 1998), the QV curves from slow inactivated channels are shifted to more negative potentials on the voltage axis, as compared with the QV curves obtained from non–slow inactivated channels at the normal negative resting potential. In *Shaker* (Δ6-46, fast inactivation removed [Sh-IR]; Hoshi et al., 1990), the macroscopic ionic conductance decays slowly (in seconds) during long depolarizations as the channels undergo slow inactivation (Hoshi et al., 1991; López-Barneo et al., 1993). As slow inactivation develops with time, the voltage dependence of charge movement shifts towards more negative potentials (Olcese et al., 1997) as a result of a protein conformational change. In the *Shaker* Δ6-46 background (Sh-IR), the double mutation T449V-I470C (Holmgren et al., 1997) completely abolishes inactivation. Surprisingly, we found that in this mutant, despite the lack of inactivation, long depolarizations still produced a leftward shift of the QV curve as it occurs in normal inactivating chan-

Address correspondence to Dr. Enrico Stefani, UCLA School of Medicine, Department. of Anesthesiology, BH-509A CHS, Box 957115, Los Angeles, CA 90095-7115. Fax (310) 825-6649; E-mail: estefani@ucla.edu

nels. Undoubtedly, this finding points out that although the channel does not inactivate, long depolarizations still produce a conformational change that is revealed as changes in the voltage dependence of the charge movement. The evidence for this conformational change came with the identification of a new, kinetically distinct open state, which is progressively populated during depolarizations and remains conductive for a relatively long time after the membrane is repolarized. The experimental evidence that the population of this new state follows the time course of the change in voltage dependence of the charge movement during depolarization provides additional support to the hypothesis that the inactivated state has become conductive as a consequence of the T449V-I470C mutation.

MATERIALS AND METHODS

Molecular Biology and Oocyte Injection

cDNA encoding for the *Shaker* H4 K^+ channel (Kamb et al., 1987), lacking the amino acids 6–46 to remove the fast inactivation (*Shaker*-IR; Hoshi et al., 1990), and the double mutant *Shaker*-IR T449V-I470C were used for measurements of ionic and gating currents (Holmgren et al., 1997). The mRNAs were translated in vitro (mMESSAGE mMACHINE; Ambion) and injected in *Xenopus laevis* oocytes (stage V–VI). 24 h before cRNA injection, the oocytes were treated with collagenase (200 U/ml; GIBCO) in a Ca^{2+}-free solution to remove the follicular layer. Oocytes were injected with 50 nl cRNA (0.1 μg/μl) suspended in water using a Drummond nanoinjector and maintained at 18°C in modified Barth's solution containing (in mM): 100 NaCl, 2 KCl, 1.8 $CaCl_2$, 1 $MgCl_2$, 5 Na-HEPES, pH 7.6, and 50 mg/ml gentamicin.

Gating and Ionic Current Recording

Cut-Open Oocyte Voltage Clamp. Gating currents were recorded 1–5 d after injection using the cut-open Vaseline gap voltage clamp (Stefani and Bezanilla, 1998), whereas ionic currents were recorded with conventional cell-attached patch-clamp techniques. MES was the main anion in the recording external solutions. In the cut-open oocyte technique, the external solution was (in mM): 110 *N*-methylglucamine-MES (NMG-MES), 2 $Ca(MES)_2$, and 10 NMG-HEPES (isotonic NMG-MES Ca-MES 2). The internal solution contained (in mM): 110 NMG-MES, 10 NMG-HEPES, and 10 $(NMG)_2$-EGTA (isotonic NMG-MES). For gating current recording, the oocytes were K^+-depleted by long repetitive depolarizations while continuously perfused with the K^+-free solution until complete K^+ washout. Standard solution for the intracellular recording micropipet was 2,700 mM NaMES and 10 mM NaCl. Low access resistance to the oocyte interior was obtained by permeabilizing the oocyte with 0.1% saponin. Gating currents were recorded unsubtracted or using a P/−4, −6 subtracting protocol; the subtracting holding potential was 0 or −120 mV depending on the pulse protocol applied.

Patch-Clamp Recordings. For experiments in the cell-attached configuration, after removal of the vitelline membrane, macroscopic and single channel currents were recorded in a solution containing the following (in mM): 120 KMES, 10 HEPES, and 2 $CaCl_2$ for bath and pipet. Pipet resistances were 2–3 MΩ for macroscopic currents and 20–50 MΩ for single channel recordings. All recording and perfusion solutions were buffered at pH 7.0. All experiments were performed at a room temperature of 22–24°C. The filter cut-off frequency was one fifth of the sampling frequency.

Fluctuation Analysis and Conditional Open Probability

Analysis of macroscopic ionic current traces used the following relation (Sigworth, 1981):

$$P_{11}\langle t_2|t_1\rangle = \frac{C(t_1,t_2)}{iI(t_1)} + \frac{I(t_2)}{iN}. \quad (1)$$

The quantity $P_{11}(t_2|t_1)$ is the probability that a channel is open at time t_2, given that it was open at the reference time t_1. It will be referred to as conditional open probability (COP).[1] The other terms in the equation are the ensemble autocovariance function $C(t_2,t_1)$, the mean current $I(t)$, the unitary current i, and the number of channels N in the preparation.

For $t_1 = t_2$, the autocovariance function is equivalent to the variance, $P_{11}(t_2|t_1) = 1$, and Eq. 1 reduces to the well known result describing the stationary variance (Sigworth, 1980, 1981). Ensemble traces of macroscopic currents were recorded in the cell-attached mode using symmetrical 120 mM KMES solutions. Pipet resistances were between 1.1 and 1.4 MΩ. For each experiment, ensemble traces were collected for two voltage protocols. The short protocol used a depolarizing test pulse to 30 mV for 40 ms, and then returning to −100 mV. The long protocol was similar except for a test pulse duration of 300 ms. Acquisition was sampled at 50 kHz and filtered at 10 kHz for the short protocol, and sampled at 5 kHz and filtered at 1 kHz for the long protocol. Linear leak and capacity transient subtraction for the purpose of obtaining the mean ionic current was performed online using the P/−4 procedure. The procedure for obtaining the autocovariance function used pair-wise analysis of traces and was described previously (Sigg et. al., 1994). In the short pulse ensemble, 200 records were used, with <5% overall drift of the current. Analysis of groups 2, 5, and 10 did not produce any significant difference in variance. The time between pulses was 15 s at −100 mV. In the case of the Sh-IR-T449V-I470C mutant, the channel noise in the tail current was easily observable above background noise and required approximately 10 s to disappear altogether. The long pulse ensemble included 100 records for Sh-IR and 84 for Sh-IR-T449V-I470C. There was <10% overall drift of the ionic current, which again produced no noticeable difference in variance between groups of 2 and 5, and only minor changes with groups of 10.

Conditional Open Probability Analysis

Sigworth (1981) demonstrated that Eq. 1 holds for the following conditions: (1) constant membrane potential for the duration of the analysis; (2) a single conductance value for the open state; (3) discrete state Markov gating kinetics; and (4) independent and homogenous channels. The equation is valid for $t_2 > t_1$ as well as $t_2 < t_1$ as long as condition (1) is satisfied. The significance of the COP is that, for a kinetic scheme containing a single open state, the decay rate of P_{11} ($t_2 > t_1$) is independent of the initial conditions and reference time t_1. Therefore, it can be inferred that any dependence of the time course of the tail current COP decay on the test pulse duration or on t_1, is a sign of multiple open states.

Although, on the surface, single channel analysis would be the preferred method of obtaining such information, the ensemble method has several advantages. First, the data acquisition is simpler. Second, the ensemble technique samples a larger number of channels, thus, averaging out minor differences in kinetics

[1]*Abbreviations used in this paper:* COP, conditional open probability; IC, inactivated conducting; INC, inactivated nonconducting.

within the population. Last, open events may occur rarely for large reference times, which could lead to under sampling at a low open probability. For rare events, and in the absence of contaminating channels, the ensemble method has greater statistical accuracy, which is only matched by conventional single channel analysis using a very large number of records.

RESULTS

Lack of Inactivation in Sh-IR-T449V-I470C: Macroscopic and Single Channel Currents

In Sh-IR–expressing oocytes, the ionic conductance decays slowly as the channels become slow inactivated. As shown by Fig. 1 (left), long depolarizations in symmetrical K^+ conditions elicit an outward (+50 mV) or an inward (−45 mV) K^+ current that activates rapidly and partially inactivate during the 8-s pulse. At the end of the pulse, when the potential returns to the holding potential (−90 mV), the channels deactivate quickly as indicated by the fast kinetic of the tail currents. In identical conditions and during pulses of the same duration, the double mutant Sh-IR-T449V-I470C does not show ionic current inactivation (Fig. 1, right). Instead, the onset of the current (particularly at negative potentials) shows two components: a fast component with a time course very similar to the one of Sh-IR; and a second very slow component with time constants that are comparable to the ones seen for the slow inactivation in Sh-IR. For a stronger depolarization (+50 mV; Fig. 1, right), the slow component is less evident. The deactivation of the double mutant at the end of the 8-s pulse shows a much slower time course when compared with Sh-IR. The slow activation kinetics of the mutant suggests the occupancy of a new state during the pulse.

The behavior of Sh-IR-T449V-I470C currents is evident in the single channel records illustrated in Fig. 2. Although the activity of Sh-IR ceased after a few seconds because of slow inactivation (Fig. 2 A), even if the depolarization to 50 mV is maintained, in Sh-IR-T449V-I470C, the channel activity continued for the full duration of the pulse (Fig. 2 C). Moreover, after repolarization to −90 mV at the end of the long pulse, the channel activity continued for a few seconds before the channel closed. The single channel IV plot of Fig. 2 E shows that the double mutation also reduced the single channel conductance of the *Shaker* channel from 17 to 9 pS.

In the Double Mutant, the Slow Component of the Macroscopic Current during Activation at −45 mV Is Produced by Long Single Channel Openings, Not Observed in Sh-IR

As shown in Fig. 1, in the double mutant, the activation of the ionic current at −45 mV has a fast onset followed by a second slower component, suggesting that a new open state becomes populated during the depolarizing pulse. We have examined the single channel activity at this potential to determine the origin of the two components of the activation. Fig. 3 A shows that long (3.2 s) depolarizing pulses to −45 mV elicited three different modes of activity in Sh-IR-T449V-I470C. At the beginning of the depolarization, the mutant channel mainly displays brief openings (Mode 1, *). As the depolarization proceeds, a new open state, characterized by a higher open probability with some flickering (Mode 2, **), becomes populated. In some cases, the flickering activity is replaced by a long opening without flickering (Mode 3, ***; Fig. 3 A). The fact that the mean current during Modes 2 and 3 has a similar value may suggest that during Mode 3, a very fast flickering that is not resolved by the recording bandwidth may occur. These three modes of operation are well illustrated in the consecutive single channel records in Fig. 3 A. The ensemble average of 30 single channel records shown in Fig. 3 B reproduces the biphasic activation observed at the same potential in the macroscopic current records (Fig. 1 B).

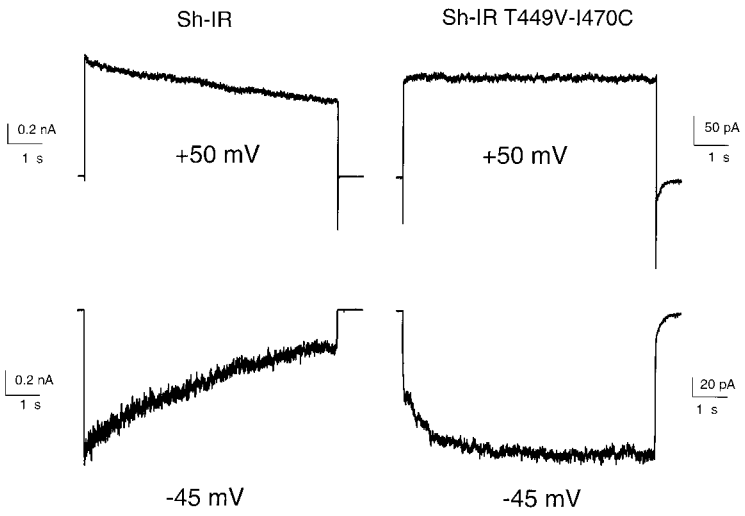

FIGURE 1. Lack of inactivation in Sh-IR-T449V-I470C macroscopic current. Ionic currents elicited by pulses of 8 s from −90 mV to the indicated potential, in Sh-IR (left) and Sh-IR-T449V-I470C (right). Current records are acquired in the cell-attached patch configuration in symmetric K^+ solutions. Note the lack of inactivation and the slow deactivation of the tail currents in Sh-IR-T449V- I470C.

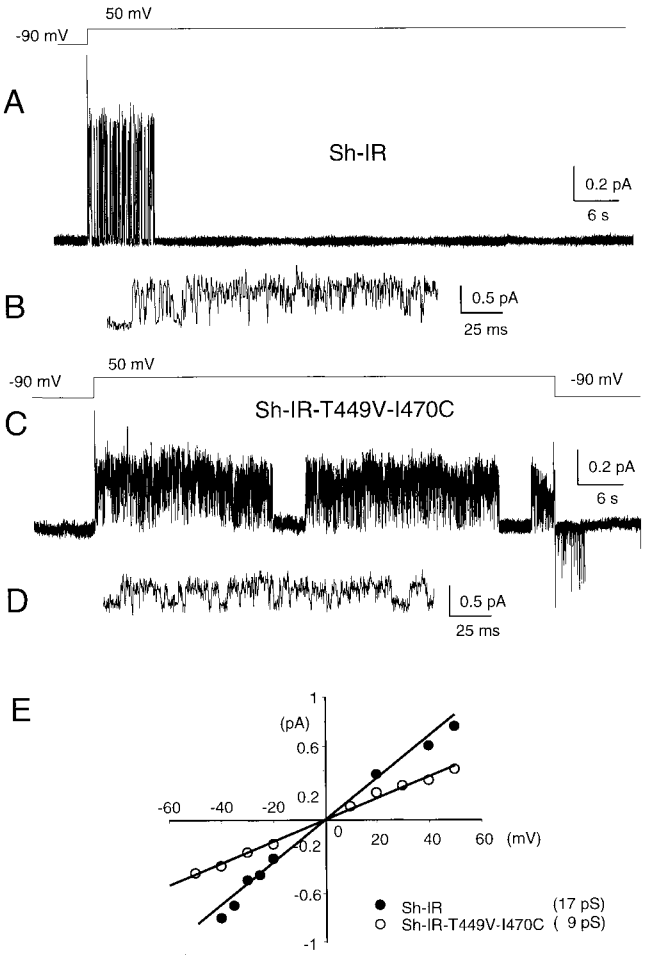

FIGURE 2. Single channel activity of Sh-IR and Sh-IR-T449V-I470C at +50 mV. Cell-attached patch recordings from oocytes expressing Sh-IR (A and B) and Sh-IR-T449V-I470C (C and D). From a holding potential of −90 mV, the membrane patches containing a single channel were depolarized to +50 mV for ~80 s (the pulse protocol is shown above the records). The channel activity in Sh-IR persisted for ~10 s before the channel fully inactivated (A). In Sh-IR-T449V-I470C (C), the channel activity was sustained throughout the depolarization and persisted for a few seconds after repolarization to −90 mV. The activity of both channels is also shown in an expanded time scale (B and D). Sh-IR was sampled at 10 kHz and filtered at 2 kHz; T449V-I470C was sampled at 5 kHz and filtered at 1 kHz. Long records are shown decimated. (E) Single channel IV plot for Sh-IR(●) and T449V-I470C (○) in symmetrical 120 mM K^+. The chord conductance calculated for Sh-IR and T449V-I470C was 17 and 9 pS, respectively.

On the other hand, in Sh-IR the single channel activity at −45 mV is characterized by brief openings that closely resemble Mode 1 of Sh-IR-T449V-I470C (Fig. 3 C). The ensemble average of Sh-IR single channel records (Fig. 3 D) produced a fast rising current, which slowly decayed as slow inactivation developed. In summary, single channel recordings of Sh-IR-T449V-I470C show at least two new classes of openings (Modes 2 and 3) with higher open probability that underlie the slow component of activation. Thus, it seems that the main effect of the double mutation is to change the kinetics of channel opening and closing. However, a closer look at the records shows that during the long opening, the channel tends to be stabilized to a somewhat lower conductance state. Brief openings during Mode 1 gating have an average peak amplitude of approximately −0.45 pA at −45 mV, as shown in the single channel I-V plot in Fig. 2 E. On the other hand, during Mode 2 gating, the channel is stabilized to an average conductance state with a lower amplitude of approximately −0.3 pA. Flickering openings during Mode 2 have a similar peak amplitude as Mode 1, but we cannot determine whether the flickering openings during Mode 2 correspond to fast transitions between Modes 1 and 2 or is an intrinsic activity during Mode 2.

During Short Depolarizations Sh-IR and Sh-IR-T449V-I470C Show Similar Properties

We compared Sh-IR and Sh-IR-T449V-I470C properties during pulses of 40-ms pulse duration. As shown in Fig. 4, both clones behave similarly during short depolarizations. The family of K^+ current traces from an oocyte expressing Sh-IR-T449V-I470C (Fig. 4 A) is practically identical to the family of current traces elicited from Sh-IR (Fig. 4 C). The tail currents that, according to Fig. 1, are expected to be slower in the double mutant after long depolarization, have a similar time course in the two clones with short depolarizing pulses (40 ms). The current-voltage relationship (IV) curves for the two clones shown in Fig. 4 (B and D) are virtually indistinguishable, suggesting that the two clones behave similarly for short pulses before the slow inactivation process develops.

Depolarized Holding Potentials Produce a Left Shift of The QV Curve in Sh-IR-T449V-I470C

Slow (C/P-type) inactivation causes a molecular rearrangement of the channel protein that leads to a nonconductive (inactivated) state. We have previously shown that in Sh-IR the midpoint of QV measured from slow inactivated channels is shifted to more negative potentials with respect to the normally hyperpolarized channel (Olcese et al., 1997), and that the shift correlates in time with the onset of slow inactivation of the ionic current. Fig. 5 (A and B) shows a family of gating currents elicited from a K^+-depleted oocyte expressing Sh-IR-T449V-I470C. The gating currents were recorded from HP = −90 (Fig. 5 A) and from HP = 0 mV (Fig. 5 B). Even though Sh-IR-T449V-I470C does not undergo slow inactivation, the QV curve obtained from gating current elicited from 0 mV HP (Fig. 5 C, closed circle) was shifted left by ~30 mV with respect to the QV curve obtained from gating current elicited from HP = −90 mV (Fig. 5 C, open circle). For comparison, Fig. 5 (D–F) shows a similar experiment for

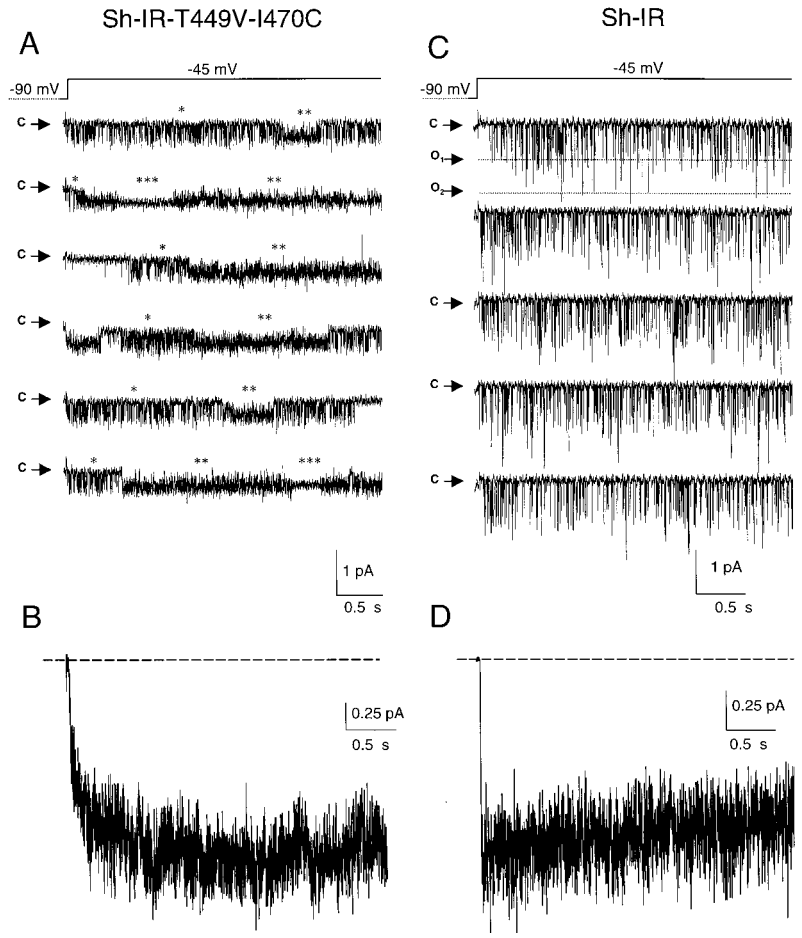

FIGURE 3. Single channel activity of Sh-IR and Sh-IR-T449V-I470C at −45 mV. (A) Consecutive recordings in a cell-attached configuration (120 mM K^+ in bath and patch pipet) from an oocyte expressing Sh-IR-T449V-I470C. The membrane patch contained a single channel. At least three patterns of opening are present: brief openings (Mode 1, *); sustained activity characterized by a higher open probability with some flickering (Mode 2, **); and long openings without flickering (Mode 3, ***). The ensemble average of 30 records from the same patch is shown in B. (C) Single channel activity in Sh-IR at −45 mV; only brief openings are present. The patch contained at least two channels. (D) Ensemble average of 40 records from a patch containing at least four channels, same oocyte as in C. The pulse protocol is shown in the top panels; arrows indicate closed (c) and the open (o) states.

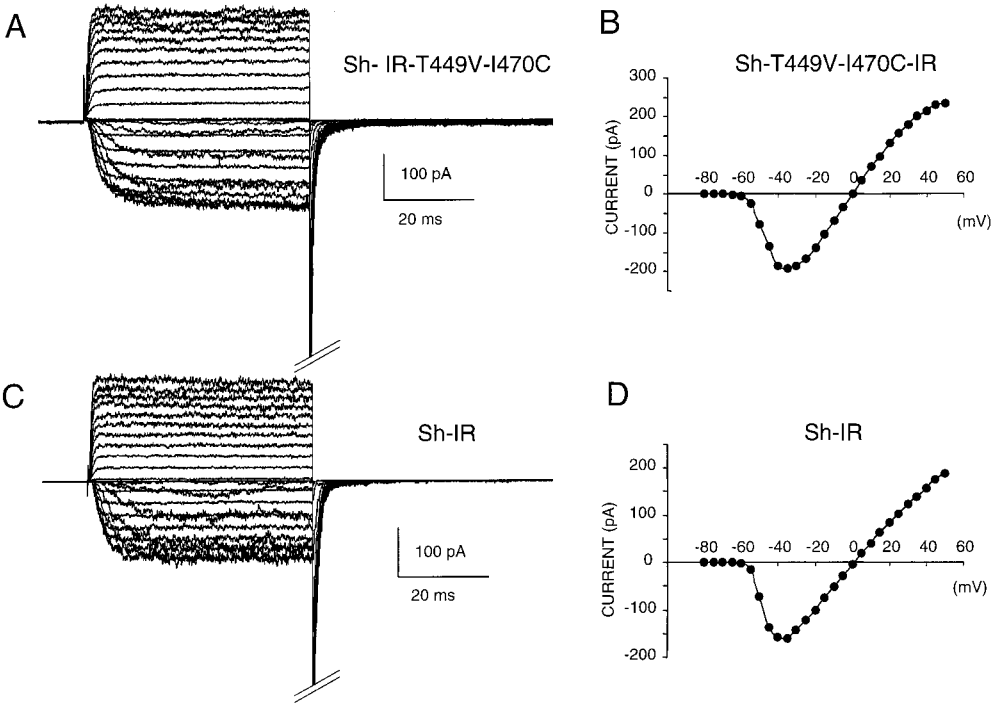

FIGURE 4. Kinetics and current-voltage relationships are practically indistinguishable in Sh-IR-T449V-I470C and Sh-IR during short depolarizations. K^+ current families from oocytes expressing (A) the double mutant Sh-IR-T449V-I470C and (C) Sh-IR evoked by 40 ms pulses ranging from −80 mV to + 50mV in 5-mV increments, from a holding potential of −90 mV. The corresponding IV curves are shown in B and D.

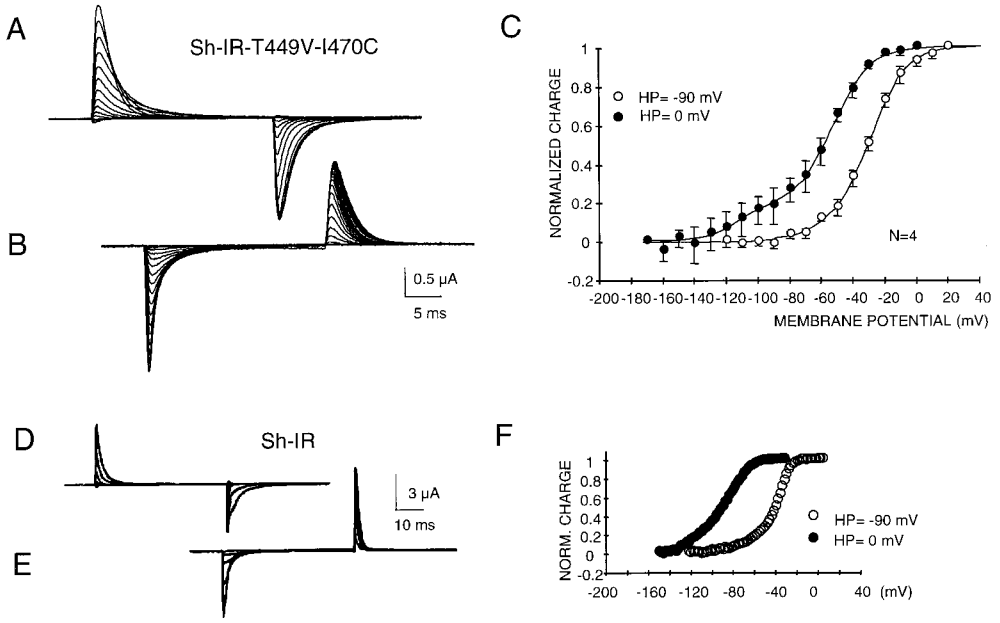

FIGURE 5. In Sh-IR-T449V-I470C and in Sh-IR, long depolarizations produce a change in the voltage dependence of charge movement. Gating currents recorded in NMG-MES solution from K^+-depleted oocytes using the cut-open oocyte voltage clamp technique. (A) Gating currents from Sh-IR-T449V-I470C recorded from −90-mV holding potential during voltage steps from −120 to 20 mV in 10-mV increments (SHP = −120 mV; $P = -4$). (B) Gating currents from the same oocyte recorded from 0-mV holding potential and during hyperpolarizations ranging from −10 to −170 mV in −10-mV increments (SHP= 0 mV, $P = -6$). The plot in C shows the time integral of the ON gating currents (QV curve) for the two holding potentials (HP = 0 mV, ●, and HP = −90 mV, ○). D and E show unsubtracted gating currents from Sh-IR in identical conditions as in A and B. The corresponding QV curves showed in F illustrate the shift to more negative potentials of the QV from slow inactivated channels (HP = 0 mV, ●, HP = −90 mV, ○).

Sh-IR. The records are gating currents from Sh-IR, from HP = −90 mV (Fig. 5 D) and from 0 mV (Fig. 5 E). As reported by Olcese et al. (1997), in slow inactivated channels (HP = 0 mV), the QV curve (Fig. 5 F, closed circle) is left-shifted on the voltage axis (∼40 mV) when compared with the QV curve constructed from gating currents from normally hyperpolarized channels (HP =−90 mV, open circle).

In Sh-IR-T449V-I470C Long Depolarizations Populate a New Open State that Is Also Revealed by a Slower Deactivation Rate

The left shift of the QV curve in Sh-IR-T449V-I470C, when the channels are held at HP = 0 mV, is an indication of a conformational change that occurs during long depolarization. However, this conformational change, which in Sh-IR leads to a nonconducting inactivated state, does not produce a reduction in current in Sh-IR-T449V-I470C (Figs. 1 and 2). Instead, as shown in Fig. 3 (A and B), two classes of openings are clearly distinguishable during depolarization to −45 mV. In Sh-IR-T449V-I470C, the population of a new state during depolarizations seems evident also in the tail current.

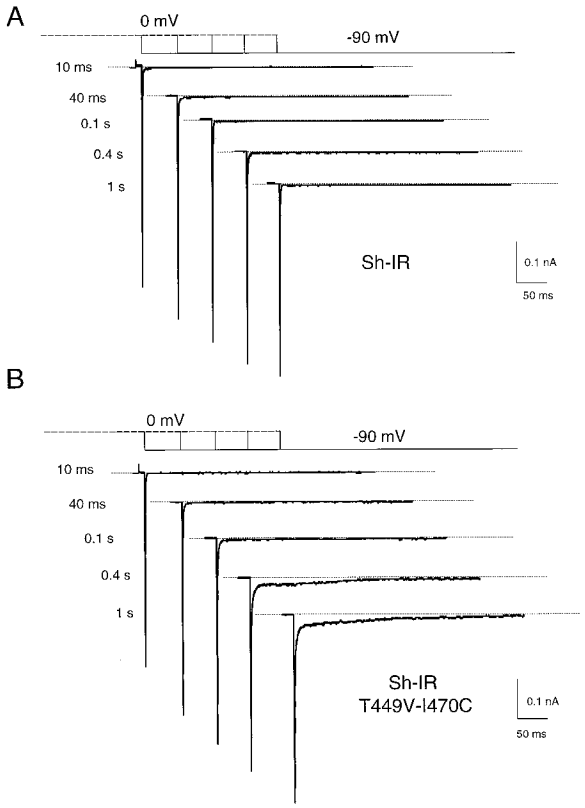

FIGURE 6. The deactivation rate of Sh-IR-T449V-I470C depends on the duration of depolarizations. The top panel shows K^+ tail currents from an oocyte expressing Sh-IR during repolarization to −90 mV. The tail currents are recorded after depolarizations to 0 mV of increasing duration (the duration of the preceding pulse to 0 mV is shown next to the traces). Note that the duration of the conditioning depolarization does not affect the rate of deactivation. In the bottom panel, the same experiment as in A but from an oocyte expressing Sh-IR-T449V-I470C. The tail currents show the appearance of a slow component that progressively increases with pulse duration.

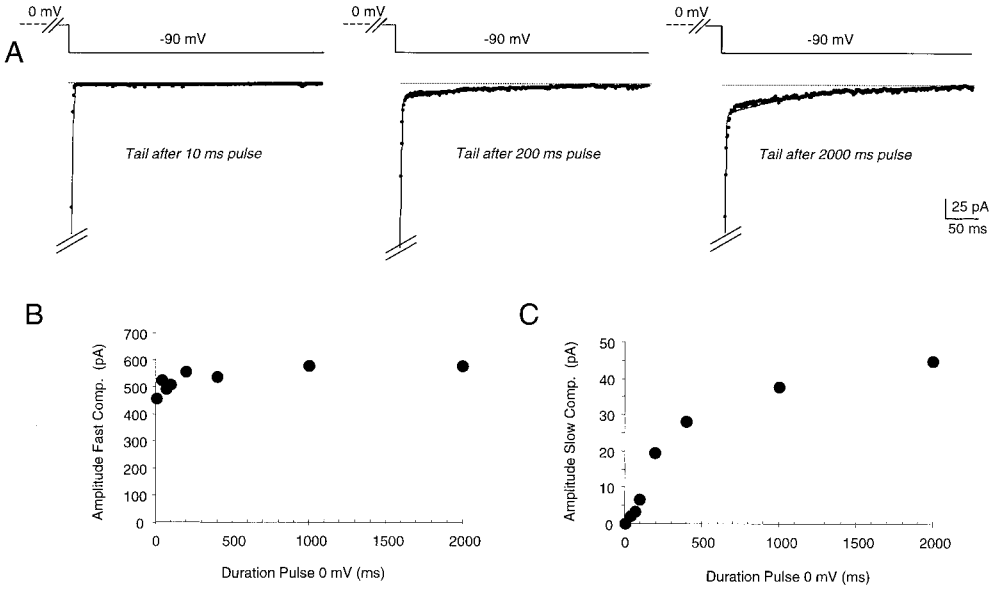

FIGURE 7. Two components in the tail current of Sh-IR-T449V-I470C. After conditioning depolarization to 0 mV for 0.01, 0.04, 0.07, 0.1, 0.2, 0.4, 1.0, and 2.0 s, the decaying phase of the tail currents at −90 mV were simultaneously fit to the sum of two exponential functions with the constraint that the two time constants were maintained in all traces. (A) Shows tail currents recorded after 10-, 200-, and 2,000-ms pulses to 0 mV with the respective fit superimposed. The fast and slow time constants common to all tail currents were 1.1 and 141.4 ms, respectively. The plot in B shows that the amplitude of the fast component (τ = 1.1 ms) remained practically unchanged with the different pulse duration. On the other hand, the amplitude of the slow component (τ = 141.4 ms; C) increased with the duration of the depolarization, whereas it was practically undetectable for the shortest depolarization (10 ms).

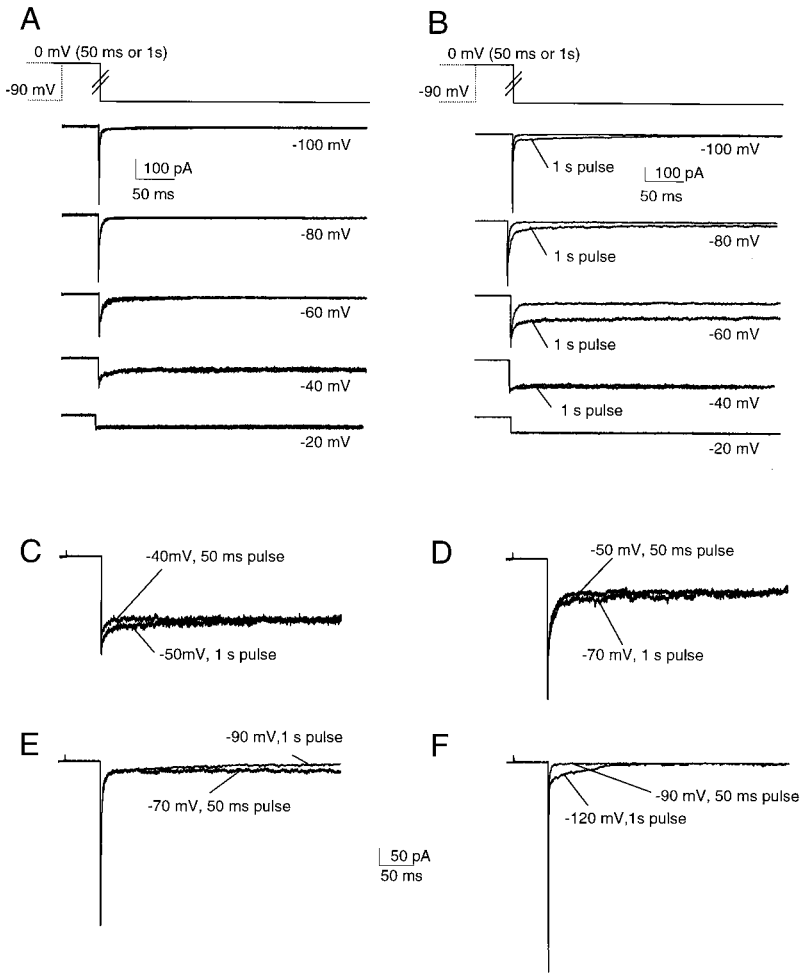

FIGURE 8. Tail currents during repolarizations at different potentials. Top panels show superimposed tail current records during repolarization to the indicated potentials, elicited after 50- or 1,000-ms pulse to 0 mV. In Sh-IR (A), the deactivation kinetics are practically identical after long (1,000 ms) or short (50 ms) depolarizations. (B) Same type of experiment as in A, but from an oocyte expressing Sh-IR-T449V-I470C. After 1,000-ms depolarizations to 0 mV, tail currents are significantly slower. (C–F) Sh-IR-T449V-I470C: superimposed deactivation tail currents at different repolarizing potentials after prepulses of 50 and 1,000 ms. Note that the voltage shift required to obtain similar time courses of deactivation tails after 50- and 1,000-ms pulses is not linear, but increases for more negative potentials.

rent. Therefore, we investigated the development of a possible slow conformational change by studying changes in tail currents as a function of the depolarizing pulse duration.

In Fig. 6, we compared tail currents in both clones during repolarization to −90 mV with preceding depolarizations of different duration. The tail currents were sampled immediately after depolarizations to 0 mV with durations ranging from 10 ms to 2 s. The top panel (Fig. 6 A) illustrates that the tail current deactivation decay rates in Sh-IR are not affected by the duration of the depolarization to 0 mV. All of the tail currents decay quickly with similar time constant when the membrane is repolarized to −90 mV, with no relationship to the duration of the depolarization. In oocytes expressing Sh-IR-T449V-I470C, the tail currents, after brief depolarizations, were fast and similar to Sh-IR (Fig. 6 B, 10-ms pulse to 0 mV). However, by increasing the duration of the depolarizations, a new slow component in the tail current becomes evident. The amplitude of the slow component of the tail current correlates with the depolarizing pulse duration, indicating that a new conducting state becomes populated during the long depolarizations. To establish the dependence of the slow component on the duration of the depolarizations, we performed a simultaneous fit of the tail current decaying phases recorded after pulses to 0 mV of 10, 40, 70, 100, 200, 400, 1,000, and 2,000 ms. All of the tail currents were fitted to the sum of two exponential functions, with the constraint that the two time constants maintained their respective values for the entire series of depolarizations. The two time constants common to all the tail currents were 1.1 and 141.4 ms. Fig. 7 A shows tail current traces at −90 mV and superimposed fits from Sh-IR-T449V-I470C for 10-, 200-, and 2,000-ms depolarizing pulses. The amplitude of the fast component (τ = 1.1 ms) is little affected by the duration of the depolarizing pulse (Fig. 7 B). On the contrary, the amplitude of the slow component (τ = 141.4 ms) depends on the duration of the depolarization (Fig. 7 C).

Negative Shift in the Voltage Dependence of Deactivation Tail Currents after Long Depolarizing Prepulses in Sh-IR-T449V-I470C

Fig. 8 (A and B) shows deactivation tail currents at different potentials for Sh-IR and Sh-IR-T449V-I470C (potentials are shown below the traces). For each potential, two tail current traces, elicited by 50- and 1,000-ms prepulses to 0 mV, are shown superimposed. In Sh-IR, the deactivation tail currents were kinetically indistinguishable for both prepulse durations. On the other hand, the double mutant, after 1,000-ms prepulse, had a slow deactivation component evident for repolarizing potentials more negative than –40 mV (Fig. 8 B). To examine whether the slower deactivation time constants after long depolarizations could be explained by the population open state with a voltage dependence shifted toward more negative potentials in respect to a

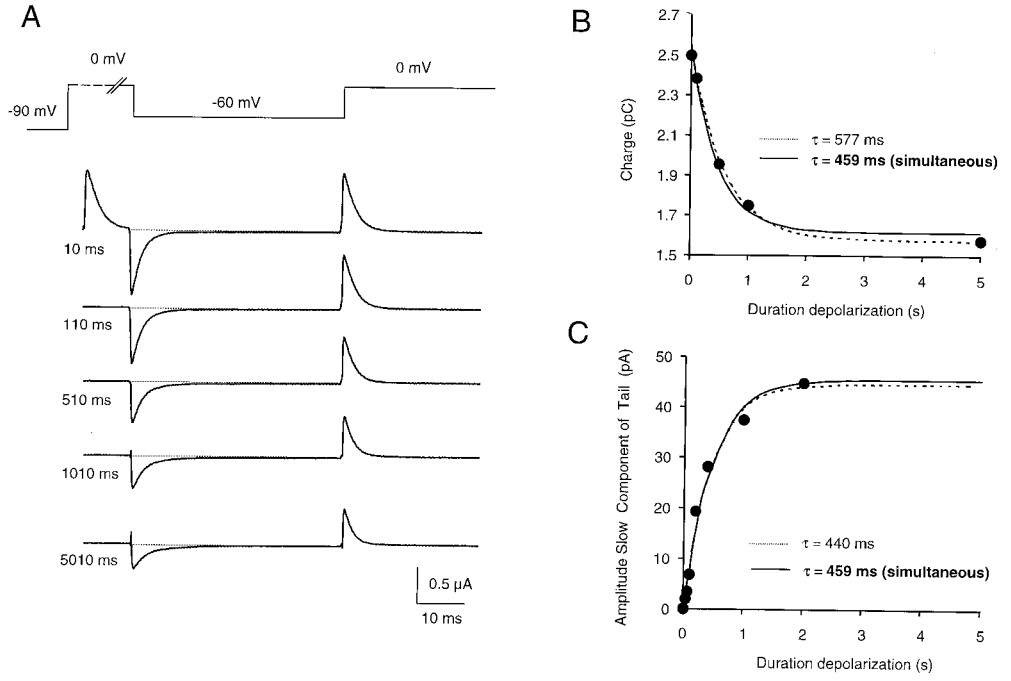

FIGURE 9. Correlation between changes in the voltage dependence of charge movement and the increase of the slow component of the tail current in Sh-IR-T449V-I470C. (A) Gating currents evoked by a voltage step from 0 mV to −60 mV recorded from a K^+-depleted oocyte (see pulse protocol in top panel). The oocyte was held at −90 mV, depolarized to 0 mV for different times (as indicated next to current traces) before the pulse to −60 mV. As shown, the gating currents were progressively reduced as the depolarization time at 0 mV increased because of the change in the voltage dependence of the charge movement. The reduction in the charge movement as a function of the duration of the depolarization is plotted in B. C shows the increase in the slow component of tail current as a function of duration of depolarization to 0 mV. Data points in B and C were fitted with single exponential functions with time constants of 557ms (B, dashed line) and 440 ms (C, dashed line). Both data sets in B and C could also be well fitted simultaneously by exponential functions with identical time constant of 459 ms (continuous lines).

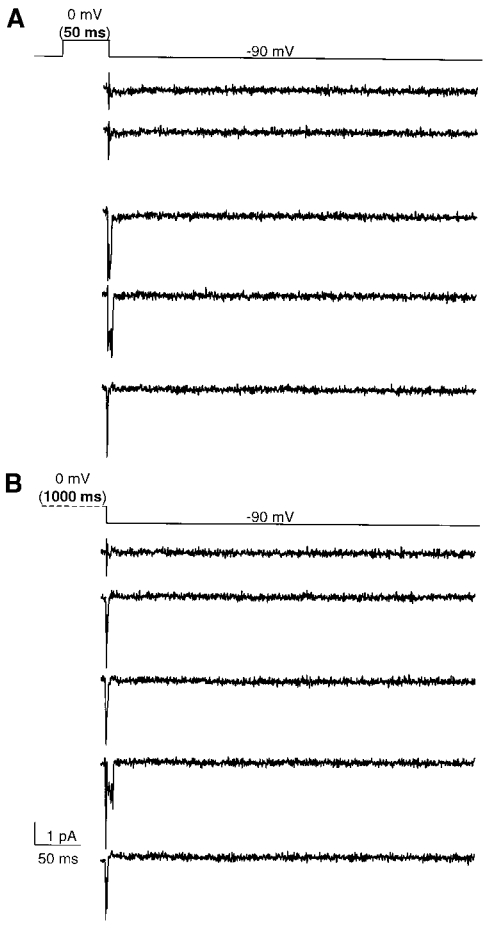

FIGURE 10. Single channel properties during deactivation in Sh-IR. The records (cell attached patch configuration) show the single channel activity at −90 mV sampled after a depolarization to 0 mV for 50 ms (A) and for 1,000 ms (B). The pulse protocol is shown above the records. Note that during repolarization, the channel activity ceased rapidly when the membrane potential returns to −90 mV for short and long pulses. Currents were sampled at 5 kHz and filtered at 1kHz.

regular open state, we compared the time course of deactivation tails at different repolarizing potentials after 50- and 1,000-ms depolarizing pulses. A rough estimate of the shift could be obtained from the repolarizing potential values at which a pair of traces with 50- and 1,000-ms prepulses had a similar deactivation time course. For example, the deactivation time course at −40 mV after a 50-ms prepulse is similar to the deactivation time course at −50 mV after the 1,000-ms prepulse (Fig. 8 C). In this case, a 10-mV shift in the voltage dependence may explain the different time course after 50- and 1,000-ms prepulses. However, the tail current kinetics at −50 mV after 50-ms depolarizing pulse, is similar to the tail current for repolarization to −70 mV after a 1-s depolarizing pulse; a larger shift, of near 20 mV was necessary to explain this difference in the time course (Fig. 8, D and E). However, as shown by the records in Fig. 8 F, a negative shift, >30 mV, would be necessary to match the kinetics of repolarizing pulses to −90 mV after 50 ms. In summary, a simple parallel shift of the voltage dependence of the new conducting state cannot explain the slower closing rate induced by long depolarizing pulses.

During Long Depolarizations, the Change in the Voltage Dependence of the Charge Movement Closely Follows the Appearance of the Slow Component in the Tail Current of Sh-IR-T449V-I470C

We have shown (Fig. 5) that the QV curves constructed from gating currents elicited from depolarized potentials (HP = 0 mV) are left shifted on the voltage axis as a result of a conformational change. The change in voltage dependence of the charge movement with long depolarizations can be monitored by changes in charge movement at a fixed potential (−60 mV) preceded by depolarizations of increasing durations. Fig. 9 A shows gating current records from an oocyte expressing Sh-IR-T449V-I470C that has been depleted of internal K^+ (see MATERIALS AND METHODS). From a holding potential of −90 mV, the membrane was depolarized to 0 mV for different time intervals and followed by a voltage step to −60 mV. Because of the change in the voltage dependence with depolarization, the amplitude of the gating currents measured at −60 mV decreases as the duration of the depolarizing pulse to 0 mV increases. The charge displaced during the voltage step from 0 to −60 mV is plotted in Fig. 9 B as a function of the depolarization time to 0 mV. The time course of the charge reduction shown in (Fig. 9 B) was fitted with a single exponential function with τ = 577 ms (Fig. 9 B, dashed line). An analogous plot in (Fig. 9 C) shows the dependence of the amplitude of the slow component of the tail current with the duration of the depolarizing pulse. The increase in amplitude of the slow component of the tail current (Fig. 9 C) could be well fitted by a single exponential with τ = 440 ms (Fig. 9 B, dashed line). Since the two processes seemed to share similar time constants we also performed a simultaneous fit of the two processes. Both sets of data (Fig. 9, B and C) could be well approximated by single exponential functions of identical time constants. The continuous lines in Fig. 9 (B and C) are the result of the simultaneous fit, showing that the two processes can be satisfactorily approximated to one exponential with a time constant of 459 ms. This finding corroborates the idea that the change in voltage dependence of the charge movement is associated with the increase in the amplitude of the slow component of the tail currents and suggests that the same process underlies the changes both in charge movement and tail currents.

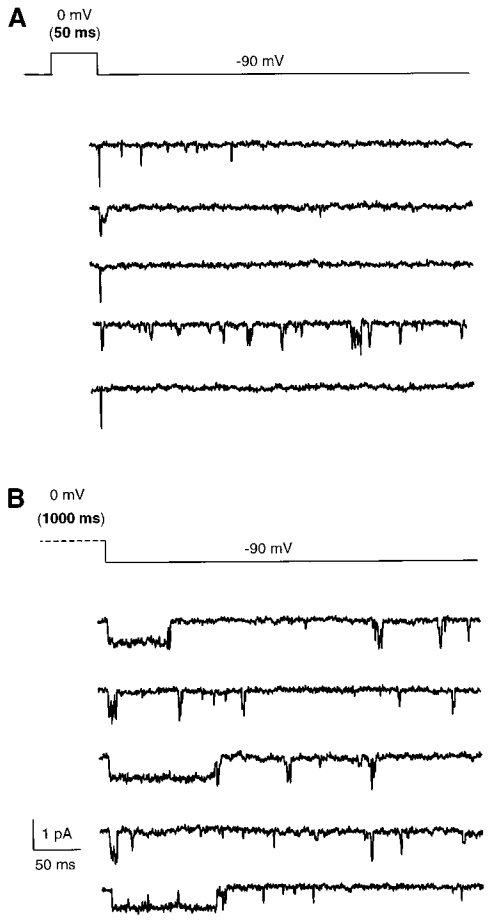

FIGURE 11. Single channel properties during deactivation in Sh-IR-T449V-I470C. The records (cell-attached patch configuration containing a single channel) show the single channel activity at −90 mV after a depolarization to 0 mV for 50 (A) and for 1,000 ms (B). Note that prolonged depolarizations stabilized a conducting state of the channel (B) that remained open for a relatively long time at −90 mV. Currents were sampled at 5 kHz and filtered at 1kHz.

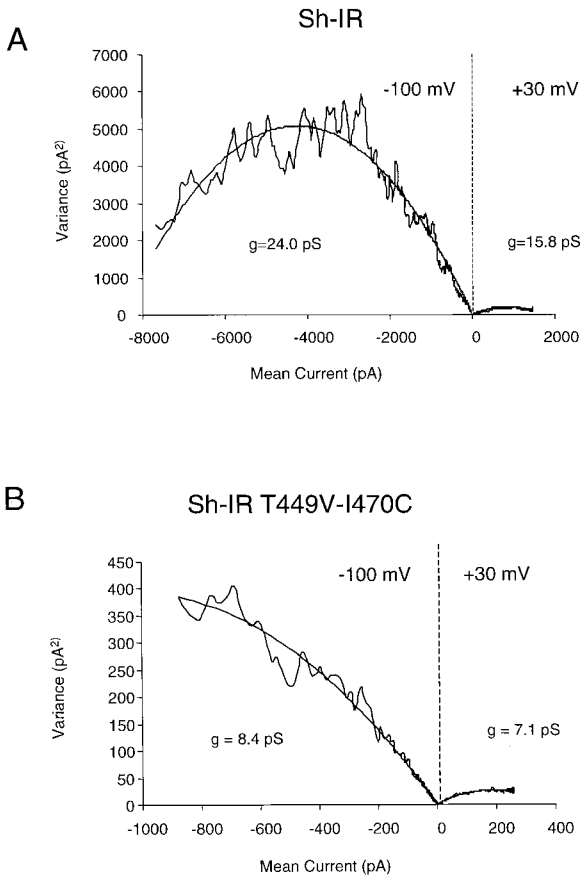

FIGURE 12. Variance-mean plot in Sh-IR (A) and Sh-IR-T449V-I470C (B). Variance-mean plots taken from an ensemble (n = 201) of current traces recorded in cell attached patch configuration and evoked by 40-ms depolarization to 30 mV, followed by repolarization to −100 mV. Depolarization and repolarization data were fit to the equation: Variance = $iI - I_2/N$, where i represents the single channel current amplitude, I is the mean current, and N is the number of channels; g is the conductance of the single channels. (A and B) are the results for Sh-IR and Sh-IR-T449V-I470C, respectively. The parameters used for the fitting were as follows. Sh-IR at −100 mV, g = 24.0, and PO_{max} 90.2%; at +30 mV, g = 15.8, PO_{max} = 87.3%, and N (at −100 and +30) = 3,538. For Sh-IR-T449V-I470C at −100 mV, g = 8.4, PO_{max} = 42.2%, and N = 2,694; at +30mV, g = 7.1 PO_{max} = 67.0%, and N = 1,380. N was estimated independently for −100 and 30 mV in Sh-IR-T449V-I470C.

In Sh-IR-T449V-I470C, a Kinetically Distinct New Open State, Populated during Long Depolarizations, Is Revealed Also during Repolarizations

In the preceding paragraphs, we have described that in Sh-IR-T449V-I470C, a slow component becomes evident in macroscopic tail currents after long depolarizing pulse duration. We have confirmed this finding with single channel recordings showing that long depolarizations to 0 mV induce the appearance of a long lasting open state during repolarizations. This new long open state was not found in Sh-IR. Single channel traces in a cell-attached membrane patch from Sh-IR are shown in Fig. 10. The current traces in (Fig. 10 A) are recorded at −90 mV after a brief depolarization (50 ms) to 0 mV. The single channel openings were all clustered at the beginning of the repolarization and lasted for a few milliseconds before the closing of the channels. Prolonging the duration of the depolarizing pulse up to 1s (0 mV; Fig. 10 B) did not change the pattern of the channel activity during the repolarization, and the channel activity ceased quickly when the potential returned to −90 mV.

A very different pattern of single channel activity was observed in Sh-IR-T449V-I470C after short and long depolarizations. Fig. 11 shows an experiment performed in identical conditions as in Fig. 10, but from a membrane patch of Sh-IR-T449V-I470C. After a short (50 ms) depolarization to 0 mV, the single channel activity at −90 mV was mainly clustered at the beginning of the repolarizing pulse and was characterized by brief openings (Fig. 11 A). In a few occasions, we could see brief

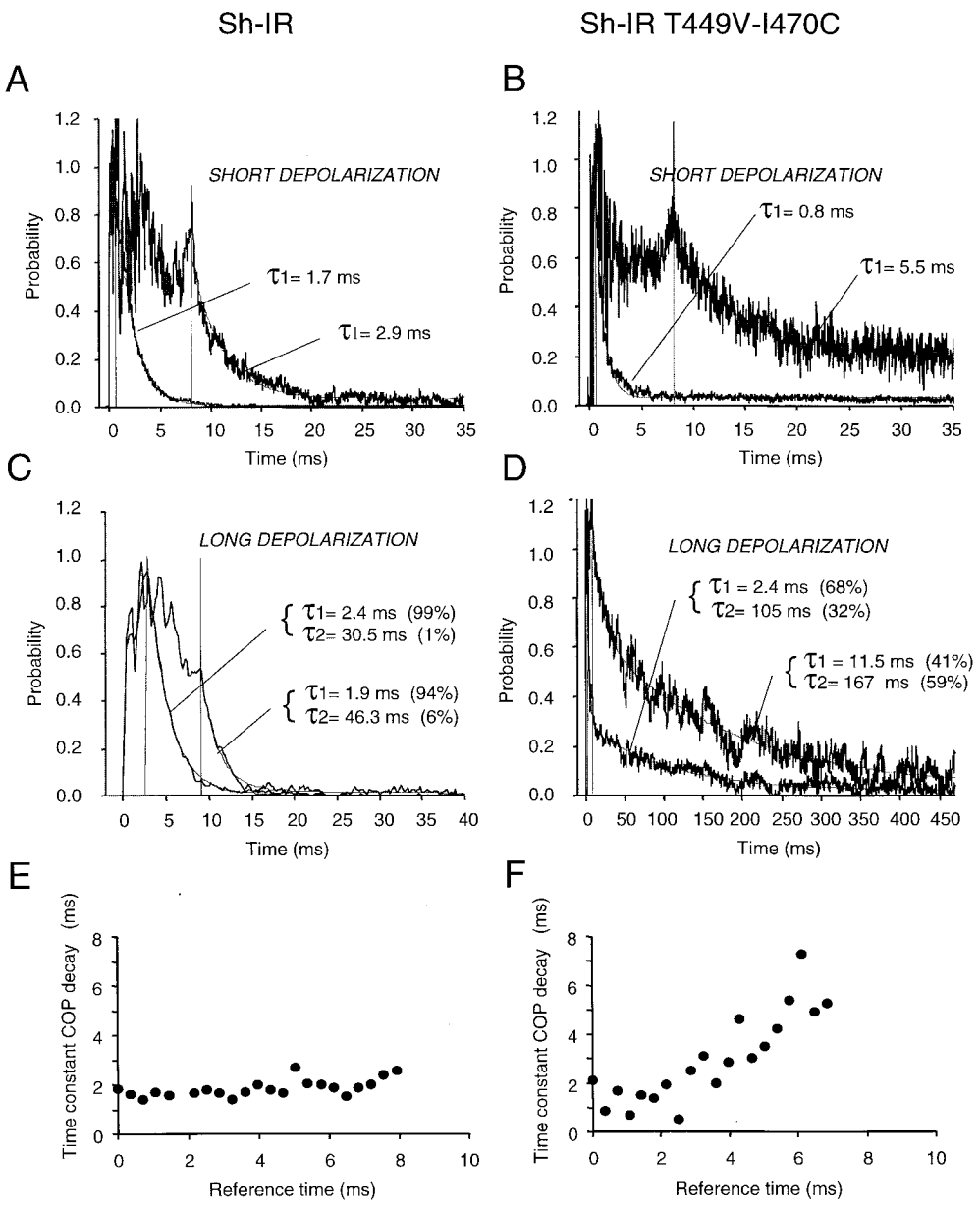

FIGURE 13. A second open state of Sh-IR-T449V-I470C revealed by conditional open probability. A–D are COP ($P(t_2|t_1)$) plots computed from ensemble of ionic tail currents using to the equation $P(t_2|t_1) = C(t_1,t_2)/iI(t_1) + I(t_2)/Ni$, where $C(t_2|t_1)$ is the autocovariance function, I(t) is the mean current, and "i" and "N" are obtained from the mean-variance analysis shown in Fig. 12. The conditional open probability at −100 mV at reference times t_1 = 0.5 and 8 ms, after a 40-ms depolarization to 30 mV, is shown for Sh-IR (A) and for Sh-IR-T449V-I470C (B). In both clones, the decays of the COP after short depolarizations (A and B) were well fitted by a single exponential function (continuous line). The time constants of the COP decay are reported in the plot. The decay of COP at −100 mV after long depolarization (300 ms) are shown in C for Sh-IR and in D for Sh-IR-T449V-I470C. Data in C and D are fitted to a sum of two exponential functions. The results of the fitting are shown in the panels. Note that, even after long depolarizations, the COP in Sh-IR decays practically monoexponentially (C) for both reference times. On the contrary, the COP in Sh-IR-T449V-I470C decays biexponentially (D). The plots in E and F show the relationship between the time constant of the COP decay with the reference time. In Sh-IR-T449V-I470C, after short depolarizing pulses, the time constant of conditional open probability decay increases quickly as a function of t_1 and pulse duration (F), an indication of the presence of more than one open state. In Sh-IR (E), the time constant of the decay is practically independent from the reference time chosen.

and long openings throughout the trace. On the other hand, at the same potential but after a longer depolarization (1 s) to 0 mV, the single channel activity was characterized by longer openings and reopenings at −90 mV (B) before the closing of the channels. These long openings are the basis for the slow component of the tail current that appears after long depolarization, as described in Figs. 6 and 7. In the context of a Markov kinetic model, a possible explanation for this result is that the mutant channel has at least a new open state that becomes progressively populated during depolarization. These findings were confirmed and quantified by the mean-variance analysis of the macroscopic currents recorded in cell attached patches.

Conditional Open Probability Analysis Reveals at least Two Open States in Shaker-IR T449V-I470C after Long Depolarizations

To calculate the number of channels in the patch and the unitary current through nonstationary mean-variance analysis (Sigworth, 1980), we selected an ensemble of macroscopic current traces suitable for analysis (see MATERIALS AND METHODS). The ionic currents were evoked by 40-ms depolarizing pulses to 30 mV,

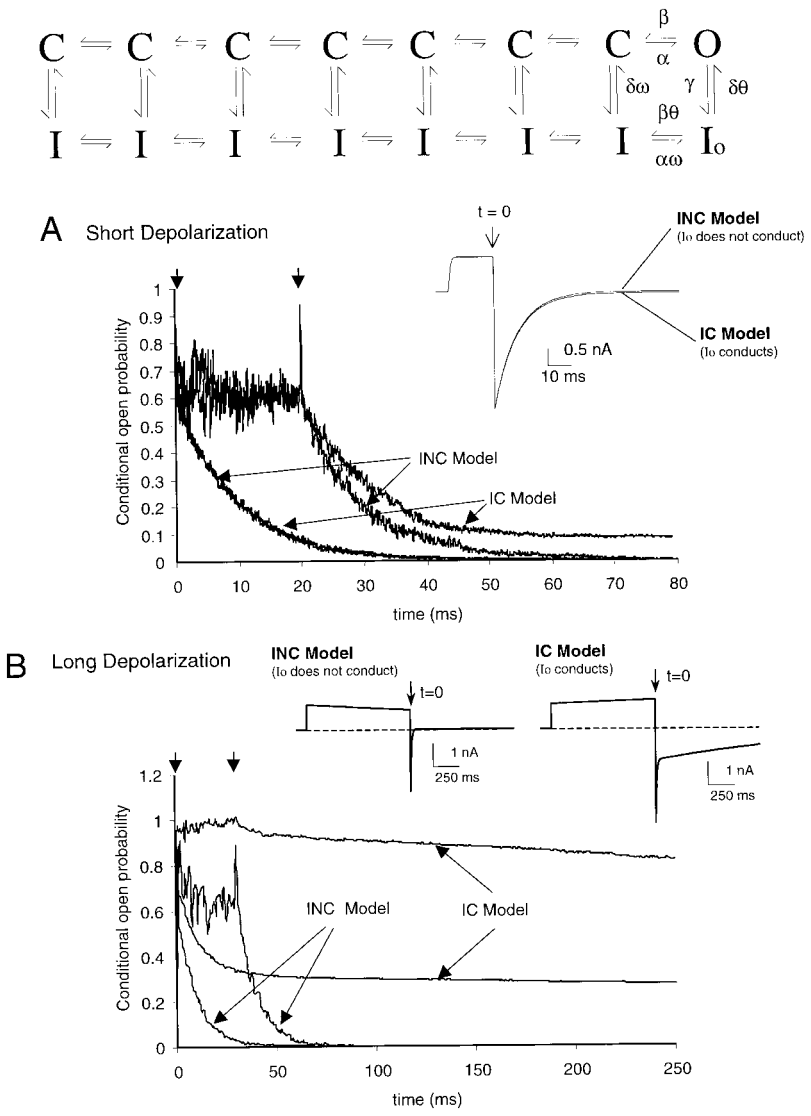

FIGURE 14. A model for Sh-IR-T449V-I470C. The model is adapted from Olcese et al. (1997), and describes equilibrium properties of slow inactivation in Sh-IR. The rate constants used for the activation pathway were identical to those in Bezanilla et al. (1994). The rate constants leading to and away from the open state (O) are, for the potential −100 mV (in ms^{-1}): $\alpha = 11.33$, $\beta = 5.23$. The voltage independent rate constants of inactivation ($\gamma = 0.00026\ ms^{-1}$, $\delta = 4.22 \times 10^{-6}\ ms^{-1}$) and the interaction energy ($\ln \omega = -2.427$ kT) are identical to the model of Olcese et al. (1997), except for the additional binding factor $\theta = 0.01$, which was added to slow transitions out of the Io state. (A) Simulated COP decay of tail currents (V = −100 mV) for the case of nonconducting inactivated state (INC), and that of conducting inactivated state (IC), after short depolarizations to 30 mV (20 ms). Two reference times are shown (see arrows) at 0.2 and 20 ms. Data were obtained from 380 groups of 5,000 accumulated runs filtered at 5 kHz, and the COP was computed according to Eq.1. (B) COP decay after a long depolarization (1 s). Data acquisition is the same as in A, except for filter rate (500 Hz). Reference times (arrows) are 2 and 30 ms. Insets show ionic current for the two models, which are similar for short depolarizations, but diverge for long depolarizations.

and were followed by repolarizations to −100 mV. The mean versus variance plots, shown for Sh-IR (Fig. 12 A) and for Sh-IR-T449V-I470C (Fig. 12 B), were fitted to the equation Variance = $iI - I^2/N$, where i is the single channel current, I is the mean current, and N is the number of channels. For Sh-IR, the best fit (Fig. 12 A, shown superimposed) gave a single channel conductance (g) of 24.0 pS at −100 mV and 15.8 pS at +30 mV, whereas for Sh-IR-T449V-I470C (Fig. 12 B), the single channel conductance was 8.4 pS at −100 mV and 7.1 pS at +30 mV. Similar values were obtained with single channel measurements at those potentials, indicating that Sh-IR has a much larger conductance at very negative potentials (Figs. 2, 10, and 11). The double mutant also displayed a reduced open probability (PO_{max}) at +30 mV when compared with Sh-IR (PO_{max} Sh-IR = 87.3%; PO_{max} Sh-IR-T449V-I470C = 67.0%).

We next computed the COP (Sigworth, 1981) for a series of reference times within the tail currents, after depolarization of 40 and 300 ms to 30 mV, using the number of channels estimated from the fit of the variance (Fig. 13). COP analysis allows the calculation of the probability that a channel is open at a certain time, given that the channel was open at one preceding reference time. The presence of multiple open states, characterized by different dwell times, can be revealed by this type of analysis and shown by a multiexponential decay of the COP. Fig. 13 A shows the tail currents COP plot in Sh-IR calculated for two reference times 0.5 and 8 ms from the beginning of the repolarization to –100 mV. As shown in Fig. 13 (A and C), the COP of the tail currents of Sh-IR decayed practically monoexponentially after short (Fig. 13 A, 40 ms) or long depolarizations (Fig. 13 C, 300 ms) with the time constant ranging between 1.7 and 2.9 ms (Fig. 13 C). No significant differences were observed for the two reference times. The

slow component is practically absent (1–6%) in Sh-IR. On the contrary, in Sh-IR-T449V-I470C, a large change in the time constant of the COP decay occurred when moving the reference time from 0.5 to 8.0 ms for both short and long depolarizations. In fact, after a brief pulse to 40 mV (Fig. 13 B), the COP calculated for reference times 0.5 and 8 ms decayed with $\tau = 0.8$ ms and $\tau = 5.5$ ms, respectively. After a long depolarization (Fig. 13 D, in milliseconds) the decay of the COP clearly became biexponential with $\tau_1 = 2.4$ ms and $\tau_2 = 105$ ms for the 0.5- ms reference time; the slow component (τ_2) was 32% of the total. Moving the reference time to 8 ms gave a COP that decayed biexponentially with $\tau_1 = 11.5$ ms and $\tau_2 = 167$; in this case, the amplitude of the slow component τ_2 increased to 59% of the total. As shown by the plot in Fig. 13 F, even after short depolarization, the time constant of the decay of COP in Sh-IR-T449V-I470C increases with increasing reference time, in contrast with the negligible changes observed for Sh-IR (Fig. 13 E).

DISCUSSION

During long depolarizations, Sh-IR channels, which possess a single open state in the activation sequence (Hoshi et al., 1994; Shoppa and Sigworth, 1998), undergo a slow reduction in macroscopic ionic conductance because of the population of slow inactivated states. The experimental results presented here indicate that the additional mutations T449V and I470C, completely abolish the inactivation (Holmgren et al., 1997) and introduce at least one additional, kinetically distinct conducting state, which populates slowly over time at depolarizing potentials. The hysteresis of the QV curves after long depolarization common to both clones (Fig. 5, C and F) can be explained by a different conformational state common to both clones that is reached at depolarized potentials and produces a new voltage dependence of the charge movement. We propose that, in Sh-IR-T449V-I470C, a process occurs that is similar to the one that produces slow inactivation in Sh-IR, but permits conduction. This hypothesis is strengthened by the experimental evidences that both the slowing down of the tail current (i.e., the population of a new state) and the shift of the voltage dependence of the charge movement (as shown in Fig. 9) share a very similar time dependence for depolarizations to 0 mV. The slower tail current deactivation rates after long depolarization could be explained by a different voltage dependence of the newly conducting state as observed in the shift of the QV curve to more negative potentials when holding at 0 mV. The transition into the new open state seems to be clearly detectable at −45 mV. In fact, at this potential, the gating shift (as the inactivation progresses) produces a large change in open probability, which is observable both in the macroscopic current as a second component in the activation (Fig. 1), and in the single channel activity (Fig. 3 A) as a change from a low to a high open probability during the pulse. Long openings are observed very frequently if the depolarizations are sustained for several seconds.

Although the presented experimental evidences show clearly the presence of at least a new open state, we applied nonstationary autocovariance analysis to better characterize Sh-IR-T449V-I470C and compared with Sh-IR. The unitary currents calculated from the variance-mean plot (Fig. 12) were similar to what was seen in the single channel experiments. The open probability (PO) of Sh-IR averaged almost 90%. On the other hand, the maximum open probability of the T449V-I470C mutant was reduced up to ∼50%. One might expect the mutant PO value to be slightly larger than that of Sh-IR if it contained more open states, even though there would be little entry into these states in the short duration (40 ms) of the depolarizing pulse. One possible explanation for the reduced open probability is that the T449V-I470C mutation enhances the presence of a blocking state connected to the regular open state (Zagotta et al., 1994). However, we did not investigate this point further.

The presence of multiple open states introduced by the T449V-I470C mutation is well revealed by the COP analysis even for short depolarizations. For a 40-ms depolarizing pulse to 30 mV, the decay was monoexponential. Reference times ranged from the start of the tail to the point at which the ionic current decayed to ∼1% of its peak value. The average rate of change of the decay time constant was ∼0.08 ms per ms of reference time for Sh-IR versus 0.72 ms per ms of reference time for the T449V-I470C mutant (Fig. 12, E and F). After a 40-ms depolarizing pulse, the approximately ninefold increase in the rate of change of COP decay in the mutant as compared with Sh-IR is suggestive of a second open state that begins to populate early, and retains probability density after the regular open state has decayed to insignificant levels.

For longer (300 ms) depolarizations, the slow inactivation of the mean ionic current has clearly developed, yet the COP decay of Sh-IR is not significantly changed as compared with the 40-ms pulse. On the other hand, there is a dramatic change in the decay rate of the Sh-IR-T449V-I470C mutant, which has developed a second, much slower component after the fast early one. The inverse relationship of COP decay rate with pulse duration and reference time is strongly suggestive of the presence of one or more open states that acquires and release probability density on a slow time scale. The results presented support the interpretation that T449V-I470C mutations convert a normally nonconductive inactivated state of Sh-IR, into a conducting state.

A Qualitative Model for Sh-IR-T449V-I470C

To test the hypothesis that in Sh-IR-T449V-I470C an inactivated state becomes conducting, we compared our results with the prediction of a published model describing slow inactivation in Sh-IR (Olcese et al., 1997). If our hypothesis was correct, we expected that, with minimal modifications, the Sh-IR model would be able to mimic the behavior of Sh-IR-T449V-I470C. As shown in Fig. 14 (top panel), the model consists of two parallel activation pathways: the top one containing seven closed states leading to the open state; and the lower one is composed of eight nonconducting inactivated states. The energy landscape of the inactivated pathway is tilted nonuniformly along the charge displacement axis with respect to the activation pathway. This occurs by virtue of a progressive stabilization of inactivated states by an energy difference: $\ln \omega = -2.42$ kT for each positive charge carrying transition (Olcese et al., 1997). The tilt in the energy landscape accounts for the shift in the apparent QV with changes in the holding potential (Fig. 5). It also ensures that the top (activation) pathway is favored at negative holding potentials, whereas the bottom inactivation pathway is populated to a progressively greater degree with depolarizing potentials. The two pathways are vertically connected by slow variables, leading to a separation of time scales between the processes of activation (horizontal movement, several milliseconds) and inactivation (vertical movement, several seconds). We have added a binding energy: $\ln \theta = -4.605$ kT to the inactivated state Io to slow the tail currents emanating from the inactivated pathway. The positive tilt in the energy landscape of the inactivated pathway could, in principle, account for the slowing of the ionic tails without the need for a separate binding energy; but, we found that a linear tilt (with respect to charge displacement) could not produce the nonuniform shift in the tail time constants seen experimentally. Thus, for this descriptive model, we found it simpler to utilize the binding energy $\ln \theta$ to slow down the tails from the Io state. The qualitative features of the kinetics obtained with the Sh-IR-T449V-I470C mutant can be reproduced simply by making conductive the inactivated state (Io) connected to the open state (O). We will refer to this model as "IC" (inactivated conducting) and we will compare it to the published Sh-IR model (Olcese et al., 1997) that will be referred to as "INC" (inactivated nonconducting).

We produced simulated ionic current traces according to the method of Clay and DeFelice (1983), and computed mean current and conditional open probability from an ensemble of accumulated traces. After brief depolarizations, the ionic tail currents of both the INC and the IC models decay with identical kinetics (Fig. 14 A, insert), though a hint of a slow component in the IC model tail current indicates that this state has begun to be populated. The effect is most noticeable in the COP decay of the IC model (Fig. 14 A). This component associated with the IC model develops with increasing reference time, whereas there is no change in COP decay in the INC model. The reason for the slowing of COP decay with lengthening reference time is due to selection bias. After enough time has developed in the tail current to depopulate the regular open state, the reference time selectively samples only the slowly decaying open inactivated state, such that the COP reflects primarily the transitions from that state.

Long depolarizations allow the inactivated state to develop more completely, making the slow component of both the ionic current tail (Fig. 14 B, inset) and the COP (Fig. 14 B) of the open inactivated state model more prominent on a long time scale. The INC model (with conventional slow inactivation) has of course fast tail currents and no change in COP decay for any time scale. The results from these simulations, together with the experimental results, suggest that T449V-I470C mutations convert at least one normally nonconductive inactivated state of Sh-IR into a conducting state.

We thank Dr. Gary Yellen for the gift of Sh-IR-T449V-I470C clone, Dr. Claudia Basso for preliminary experiments with Sh-IR-T449V-I470C, and Dr. Trude Haug for helpful comments to the manuscript.

This work was supported by National Institutes of Health grant GM52203 to E. Stefani, by the National Institutes of General Medical Sciences grant GM30376 to F. Bezanilla, and by Chilean grants FONDECYT 1000-0890, Cátedra Presidencial, and a Human Frontier in Science Program grant to R. Latorre. The Centro de Estudios is a Millenium Institute.

Submitted: 7 August 2000
Revised: 4 December 2000
Accepted: 2 January 2001

REFERENCES

Basso, C., P. Labarca, E. Stefani, O. Alvarez, and R. Latorre. 1998. Pore accessibility during C-type inactivation in *Shaker* K^+ channels. *FEBS Lett.* 429:375–380.

Bezanilla, F., R.E. Taylor, and J.M. Fernandez. 1982. Distribution and kinetics of membrane dielectric polarization. I. Long-term inactivation of gating currents. *J. Gen. Physiol.* 29:21–40.

Bezanilla, F., E. Perozo, and E. Stefani. 1994. Gating of *Shaker* K^+ channels: II. The components of gating currents and a model of channel activation. *Biophys. J.* 66:1011–1021.

Brum, G., and E. Rios. 1987. Intramembrane charge movement in frog skeletal muscle fibres. Properties of charge 2. *J. Physiol.* 387: 489–517.

Clay, J.R., and L.J. DeFelice. 1983. Relationship between membrane excitability and single channel open-close kinetics. *Biophys. J.* 42: 151–157.

De Biasi, M., H.A. Hartmann, J.A. Drewe, M. Taglialatela, A.M. Brown, and G.E. Kirsch. 1993. Inactivation determined by a single site in K^+ pores. *Pflügers Arch.* 422:354–363.

Fedida, D., R. Bouchard, and F.S.P. Chen. 1996. Slow gating charge immobilization in the human potassium channel Kv 1.5 and its prevention by 4-aminopyridine. *J. Physiol.* 494:377–387.

Holmgren, M., P.L. Smith, and G. Yellen. 1997. Trapping of organic

blockers by closing of voltage-dependent K^+ channels: evidence for a trap door mechanism of activation gating. *J. Gen. Physiol.* 109:527–535.

Hoshi, T., W.N. Zagotta, and R.W. Aldrich. 1990. Biophysical and molecular mechanisms of *Shaker* potassium channel inactivation. *Science.* 250:533–538.

Hoshi, T., W.N. Zagotta, and R.W. Aldrich. 1991. Two types of inactivation in *Shaker* K^+ channels: effects of alterations in the carboxy-terminal region. *Neuron.* 7:547–556.

Hoshi, T., W.N. Zagotta, and R.W. Aldrich. 1994. *Shaker* potassium channel gating. I: Transitions near the open state. *J. Gen. Physiol.* 103:249–278.

Iverson, L.E., and B. Rudy. 1990. The role of divergent amino and carboxyl domains on the inactivation properties of potassium channels derived from the *Shaker* gene of *Drosophila. J. Neurosci.* 10:2903–2916.

Kamb, A., L.E. Iverson, and M.A. Tanouye. 1987. Molecular characterization of *Shaker*, a *Drosophila* gene that encodes a potassium channel. *Cell.* 50:405–413.

Liu, Y., M.E. Jurman, and G. Yellen. 1996. Dynamic rearrangement of the outer mouth of a K^+ channel during gating. *Neuron.* 16: 859–867.

Loots, E., and E.Y. Isacoff. 1998. Protein rearrangements underlying slow inactivation of the *Shaker* K^+ channel. *J. Gen. Physiol.* 112: 377–389.

López-Barneo, J., T. Hoshi, S.H. Heinemann, and R.W. Aldrich. 1993. Effects of external cations and mutations in the pore region on C-type inactivation of Shaker potassium channels. *Receptors and Channels.* 1:61–71.

Ogielska, E.M., and R.W. Aldrich. 1998. A mutation in S6 of *Shaker* potassium channel decreases the K^+ affinity of an ion binding site revealing ion–ion interactions in the pore. *J. Gen. Physiol.* 112:243–257.

Ogielska, E.M., and R.W. Aldrich. 1999. Functional consequences of a decreased potassium affinity in a potassium channel pore–ion interactions and C-type inactivation. *J. Gen. Physiol.* 113:347–358.

Ogielska, E.M. Zagotta, W.N. Hoshi, T. Heinemann, S.H. Haab, and R.W. Aldrich. 1995. Cooperative subunit interactions in C-type inactivation of K channels. *Biophys. J.* 69:2449–2457.

Olcese, R., R. Latorre, L. Toro, F. Bezanilla, and E. Stefani. 1997. Correlation between charge movement and ionic current during slow inactivation in *Shaker* potassium channels. *J. Gen. Physiol.* 110:579–589.

Panyi, G., Z. Sheng, and C. Deutsch. 1995. C-type inactivation of a voltage-gated K^+ channel occurs by a cooperative mechanism. *Biophys. J.* 69:896–903.

Shirokov, R., R. Levis, N. Shirokova, and E. Rios. 1992. Two classes of gating current from L-type Ca channels in guinea pig ventricular myocytes. *J. Gen. Physiol.* 99:863–895.

Shirokov, R., G. Ferreira, J. Yi, and E. Rios. 1998. Inactivation of gating currents of L-type calcium channels. Specific role of the $\alpha 2\delta$ subunit. *J. Gen. Physiol.* 111:807–823.

Shoppa, N.E., and F.J Sigworth. 1998. Activation of *Shaker* potassium channels. *J. Gen. Physiol.* 111:271–294.

Sigg, D., E. Stefani, and F. Bezanilla. 1994. Gating current noise produced by elementary transitions in Shaker potassium channels. *Science.* 264:578–582.

Sigworth, F.J. 1980. The variance of sodium current fluctuations at the node of Ranvier. *J. Physiol.* 307:97–129.

Sigworth, F.J. 1981. Covariance of nonstationary sodium current fluctuation at the node of Ranvier. *Biophys. J.* 34:111–133.

Stefani, E., and F. Bezanilla. 1998. The cut open oocyte voltage clamp technique. *Methods Enzymol.* 293:300–318.

Yang, Y., Y. Yan, and F.J. Sigworth. 1997. How does the W434F mutation block current in *Shaker* potassium channels? *J. Gen. Physiol.* 109:779–789.

Yellen, G., D. Sodickson, T.Y. Chen, and M.E. Jurman. 1994. An engineered cysteine in the external mouth of a K^+ channel allows inactivation to be modulated by metal binding. *Biophys. J.* 66: 1068–1075.

Zagotta, W.N., T Hoshi, and R.W. Aldrich. 1994. *Shaker* potassium channel gating. III: Evaluation of kinetic models for activation. *J. Gen. Physiol.* 103:321–362.